

Proceedings

A New Granular Column Collapse Device to Characterise Flowability of Bulk Materials [†]

Joel Torres-Serra ¹, Enrique Romero ^{2,*} and Antonio Rodríguez-Ferran ²

¹ Técnicas Mecánicas Ilerdenses SL, Polígono Industrial Camí dels Frares, c. Alcarràs, parc. 66, 25190 Lleida, Spain; j.torres@tmipal.com

² Universitat Politècnica de Catalunya BarcelonaTech, Department of Civil and Environmental Engineering, c. Jordi Girona 1-3, Campus Nord UPC, 08034 Barcelona, Spain; antonio.rodriguez-ferran@upc.edu

* Correspondence: enrique.romero-morales@upc.edu; Tel.: +34-934-016-888

† Presented at the 18th International Conference on Experimental Mechanics, Brussels, Belgium, 1–5 July 2018.

Published: 26 June 2018

Abstract: A wide range of bulk materials with different physical properties are nowadays handled in the packaging industry using different material conveying techniques. Nevertheless, experimental methodologies to characterise flowability of granular materials in actual handling conditions are still under development. This paper presents a new fully instrumented device for flowability assessment by granular column collapse of bulk materials. The generated granular flow is monitored by load cells that register the flow heights and by a high-speed video camera that captures the bulk flow kinematics through particle image velocimetry analysis. The 3D surface morphology of the final condition is determined with a 2D laser profile scanner. Results show the effect of varying the initial column aspect ratio on flow response.

Keywords: granular column collapse; flowability; bulk materials; particle image velocimetry

1. Introduction

A variety of material conveying techniques are used for bulk material handling, which range from air fluidization to discharge through a hopper. Also, a wide range of powders and grains are handled in packaging operations, produced by different industrial sectors and including diverse physical properties (particle size and shape, bulk compressibility, hygroscopicity). Flowability of powders and bulk solids is fundamental in selecting adequate equipment and design strategies in order to improve their efficiency, thus yielding financial and environmental benefits. However, the industry is lacking a robust approach to the characterisation of mass flow phenomena. Therefore, a new insight into the mechanical behaviour of industrial granular flows is presented, based on a new testing device instrumented with different visualisation techniques.

We have developed and calibrated a prototype to assess flowability of powders and bulk solids by granular column collapse tests [1,2]. The experimental set-up consists of a container where a granular pile is formed, and which is then instantaneously released letting the granular material flow under gravity, as shown in Figure 1. Since the motion is governed by particle-particle interactions [3], the test provides direct observation of the kinematics of dense and dilute flow regimes generated during bulk handling [4].

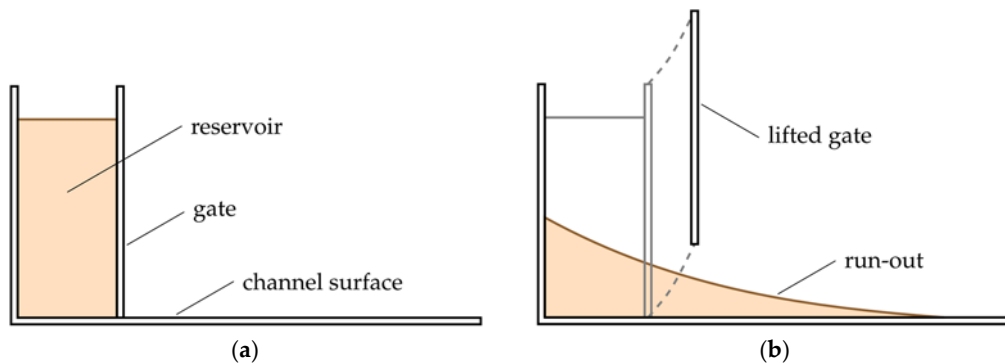


Figure 1. Quasi-2D granular column collapse test set-up schematic with a horizontal channel and a lifting gate: (a) initial configuration; (b) final deposit.

2. Materials and Methods

Figure 2 presents the testing device consisting of a channel of rectangular cross-section (1), of length 2150 mm and width 160 mm, with a horizontal anodised aluminium surface and vertical glass walls where the flow takes place. A gate is closed at a distance of 150 mm, forming a prismatic reservoir (3) where granular piles up to a height of 350 mm are prepared. The lightweight lifting gate (2) is made of carbon fibre reinforced polymer held together by a 3D-printed polymeric frame and reinforced with an aluminium sheet. The motion of the gate is controlled by a parallelogram mechanism (9) automated by pneumatic cylinders.

A permeable polyester needle-punched felt layer is placed at the reservoir base (4), preventing fine particles from entering the air chamber beneath (5), and allowing for fluidisation and deaeration of the granular pile prior to gate lifting. Different initial packing conditions are imposed:

- Poured random packing by free fall settling of the granular material into the reservoir;
- Loose packing by fluidisation, injecting a dried compressed air flow to a poured packing with velocities between minimum fluidisation and bubbling [5];
- Dense packing by deaeration, reversing the fluidisation system to impose suction by means of a vacuum ejector.

A panel including an air flow meter and two pressure switches (6) controls the pressure drop across the granular column depending on the applied air flow velocities.

The channel base is equipped with nine logarithmically-spaced moulded silicone membranes (7) mounted on beam load cells (Modelo 104, UTILCELL, Barcelona, Spain) for real-time monitoring of the flowing heights based on the load distribution along the channel surface during the flow. A panel (8) is used for signal conditioning of the force transducers. In addition, an auxiliary structure holds a linear guide with positioning control (10), where a 2D laser profile sensor (GOCATOR 2150, LMI Technologies Inc, Burnaby, Canada) is attached. The laser scanner (11) captures the 3D free surface morphology of the final deposit along the channel length. Furthermore, a high-speed video camera (PXW-FS5, SONY Corporation, Tokyo, Japan) mounted on a support (12) is used together with LED panel lights (13) to obtain lateral visualisations of the bulk flow kinematics at rates between 100 and 400 fps. Finally, a desktop computer (14) is used for data acquisition and control.

Experiments with granular piles initially at poured random packing conditions are performed using white linear low-density polyethylene (LLDPE) pellets. Properties are summarised in Table 1. Initial aspect ratios—given by the ratio of initial column height, h_0 , to fixed column base length, $l_0 = 150$ mm—range between 0.97 and 2.03, corresponding to initial column heights $h_0 = 145$ mm and $h_0 = 304$ mm, respectively.

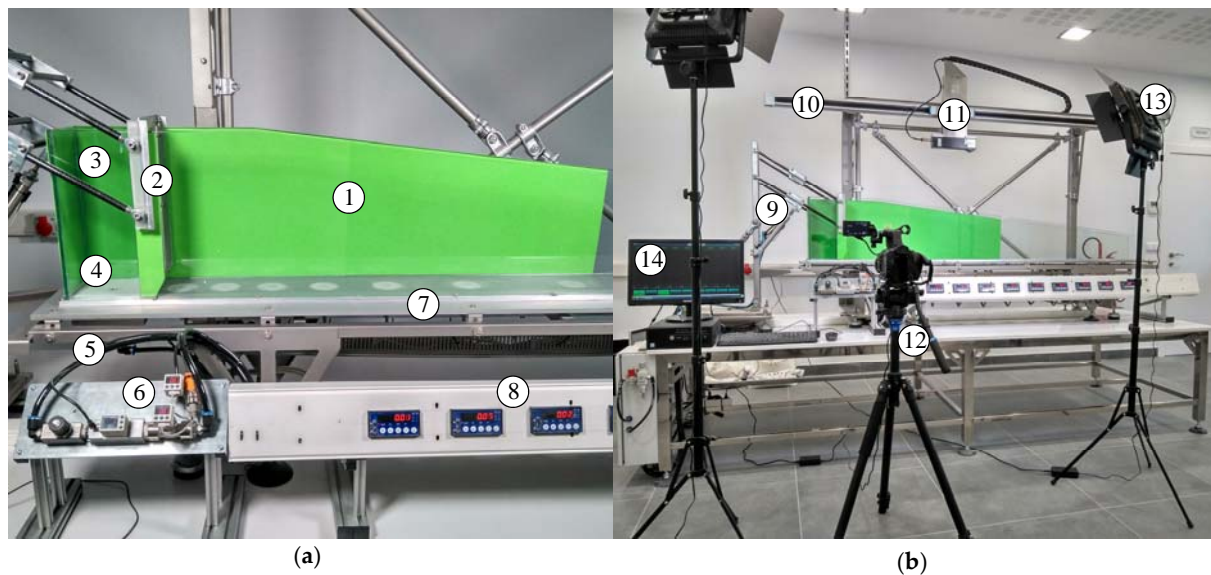


Figure 2. Photographs of the new fully instrumented prototype with numbered parts. (a) Close-up view of the channel: (1) channel with glass walls; (2) lifting gate frame; (3) reservoir; (4) porous plate; (5) air chamber; (6) air flow and pressure control panel; (7) membranes and beam load cells; (8) load cell signal conditioning panel. (b) General view of the device: (9) automated parallelogram mechanism of lifting gate; (10) linear guide with positioning control; (11) 2D/3D laser profile sensor; (12) high-speed video camera on tripod; (13) LED illumination; (14) PC for data acquisition and control.

Table 1. Physical properties of the particles used in the experiments (white particles and grey markers¹⁾.

Material	Particle Density (kg m ⁻³)	Bulk Density (kg m ⁻³)	Particle Diameter (mm)	Particle Shape (Circularity)
LLDPE pellets (white)	965	599	4.6	0.84
LLDPE markers (grey)	900	611	3.6	0.86

¹ Grey LLDPE pellets with similar physical properties are added at low mass fraction, since white LLDPE pellets have insufficient inherent texture to allow cross-correlation of the pairs of video frames analysed using PIV.

3. Results and Discussion

3.1. Flow Front Advance and Flowing Heights

Figure 3 shows the time evolution of the load cells for the two column aspect ratios. Similar flow advancing responses are observed at the beginning during downward acceleration. Flow front is detected at similar elapsed times by the three initial load cells ($L = 225$ mm, 320 mm and 425 mm in the figure), around $t = 0.35$ s for the first load cell. Nevertheless, different behavioural features are detected in the time evolutions that depend on the initial aspect ratio. For $h_0/l_0 = 0.97$, loads increase monotonically until they stabilise at the flowing heights corresponding to the final deposit. However, for $h_0/l_0 = 2.03$ a force peak of 12 mN is registered by the first load cell, before gradually approaching the final flow height at 9.3 mN. The second load cell shows a similar trend, but the effect is not detected by the subsequent load cells (Figure 3b). Flow height peaks can be attributed to vertical accelerations at the beginning for higher h_0/l_0 values, resulting in an impulse that is lost as the horizontal propagation along the channel becomes dominant.

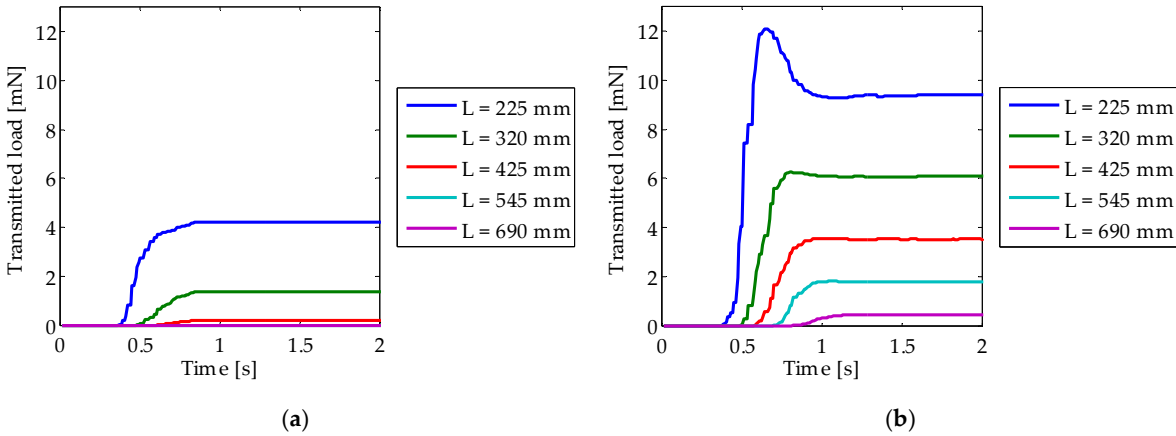


Figure 3. Flow front and deposit height estimation by real-time monitoring of beam load cells at different channel distances, L : (a) $h_0/l_0 = 0.97$; (b) $h_0/l_0 = 2.03$.

3.2. Surface Morphology of the Deposit

Different shape parameters can be quantified from the final deposit morphologies shown in Figure 4. The column with $h_0/l_0 = 0.97$ develops a deposit with height $h_\infty = 131$ mm (at $y = 0$ in the figure) and run-out length $l_\infty = 328$ mm –defined as the maximum length for which the average height along the channel width is larger than one particle diameter. The final aspect ratio is $h_\infty/l_\infty = 0.40$. In the case of $h_0/l_0 = 2.03$, the final aspect ratio is $h_\infty/l_\infty = 0.26$ ($h_\infty = 167$ mm and run-out length $l_\infty = 630$ mm). In addition, the angle of repose is of interest, and different angles can be measured along the free surface of the deposits. For $h_0/l_0 = 0.97$, the angle of repose with respect to the channel plane ranges from 12° to 25° , measured respectively at the toe and the head of the deposit. In the case of $h_0/l_0 = 2.03$, the angle of repose varies from 6.5° to 23° . The initial aspect ratio is observed to affect the final aspect ratio and the lower angle of repose of the deposit.

Moreover, the quasi-2D assumption on the experimental set-up is checked by the scanned 3D surface morphologies since the granular material is evenly distributed across the channel section for both h_0/l_0 configurations.

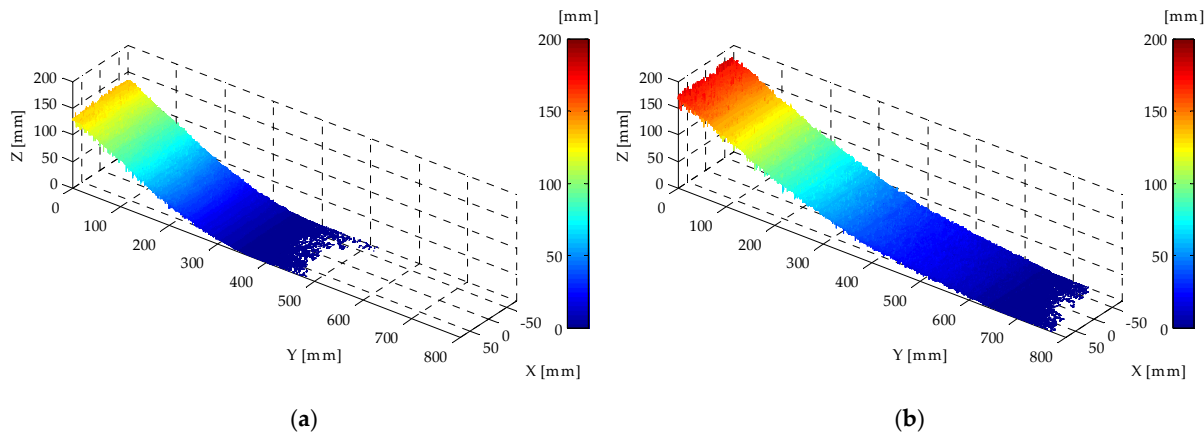


Figure 4. 3D free surface morphology of final deposits: (a) $h_0/l_0 = 2.03$; (b) $h_0/l_0 = 0.97$.

3.3. Bulk Flow Kinematics

Figure 5 illustrates the image analysis of a video frame pair, obtained from Video S1 recorded at 200 fps, and the instantaneous velocity field obtained by particle image velocimetry (PIV) using the open-source software PIVlab [6]. A mixture at 10% mass fraction of grey LLDPE marker particles is used, as can be seen in Figure 5a. Properties of these marker particles are indicated in Table 1. The kinematics of the generated mass flows is investigated from the 2D displacement and velocity vector

fields measured from the visualisations of the bulk flow through the prototype walls. In addition, the lateral contour can also be tracked during the flow and the final deposit height and run-out length validated with the laser profile sensor results.

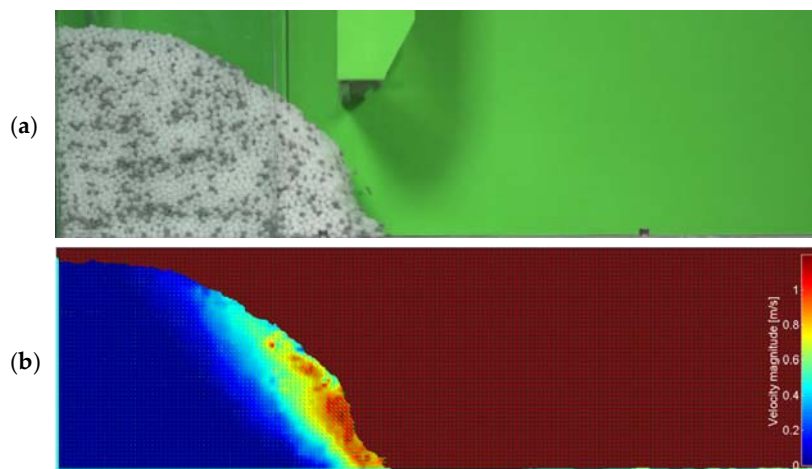


Figure 5. PIV analysis of collapse of a column of a mixture of LLDPE pellets (white) at 10% mass fraction of similar LLDPE pellets (grey) of initial column aspect ratio $h_0/l_0 = 0.97$ at time $t = 375$ ms after the onset of flow: (a) video frame; (b) velocity magnitude vector field.

4. Conclusions

We have described a new prototype to assess flowability of bulk materials by granular column collapse tests. The results provide a deep insight into the flow properties of powders and grains by means of real-time monitoring of the flowing heights, the surface morphology of the final deposit, as well as the displacements and velocities generated during the flow. This information allows characterising the dense and dilute flow regimes of granular materials found in actual bulk handling conditions. Therefore, our testing device can help decision makers to overcome qualitative estimations of flowability when selecting and designing bulk handling equipment.

We are currently developing a bulk material database including physical and mechanical properties measured using our new testing device in order to classify powders and grains based on their flowability using cluster analysis. The database will be completed with experimental results on the hydro-mechanical behaviour of the materials by granular column collapse at different initial moisture contents controlled by relative humidity [7]. Furthermore, calibrated model parameters for discrete element simulations using our experimental results will be also included in the database, with a focus on the effects of particle polydispersity [8], non-spherical particle shape, and hygroscopicity on the flow.

Supplementary Materials: Video S1: Flow generated from the release of a granular column ($h_0/l_0 = 0.97$) of poured random packing. Mixture of white LLDPE pellets at 10% mass fraction of grey LLDPE marker pellets. The video in MP4 format is originally recorded at 200 fps and displayed at 50 fps. Available online at: <https://www.dropbox.com/sh/w3zostqjmwdtalu/AACkWt0y6lbM-sss0mNjY2uQa?dl=0>.

Acknowledgments: The authors would like to acknowledge the financial support provided by Project 2014 DI 075, *Optimization of dosing systems for bulk solids using experimental and numerical techniques*, funded by the Industrial Doctorates Plan of the Government of Catalonia.

Author Contributions: All authors conceived and designed the experiments; J.T. performed the experiments and analysed the data, with the supervision of E.R. and A.R. All authors discussed and interpreted results, and commented on the paper.

Conflicts of Interest: The authors declare no conflict of interest.

References

1. Lube, G.; Huppert, H.E.; Sparks, R.S.J.; Hallworth, M.A. Axisymmetric collapses of granular columns. *J. Fluid Mech.* **2004**, *508*, 175–199, doi:10.1017/S0022112004009036.
2. Warnett, J.M.; Denissenko, P.; Thomas, P.J.; Williams, M.A. Collapse of a granular column under rotation. *Powder Technol.* **2014**, *262*, 249–256, doi:10.1016/j.powtec.2014.04.030.
3. Lajeunesse, E.; Mangeney-Castelnau, A.; Vilotte, J.P. Spreading of a granular mass on a horizontal plane. *Phys. Fluids* **2004**, *16*, 2371–2381, doi:10.1063/1.1736611.
4. Forterre, Y.; Pouliquen, O. Flows of Dense Granular Media. *Annu. Rev. Fluid Mech.* **2008**, *40*, 1–24, doi:10.1146/annurev.fluid.40.111406.102142.
5. Roche, O. Depositional processes and gas pore pressure in pyroclastic flows: an experimental perspective. *Bull. Volcanol.* **2012**, *74*, 1807–1820, doi:10.1007/s00445-012-0639-4.
6. Thielicke, W.; Stamhuis, E.J. PIVlab—Towards User-friendly, Affordable and Accurate Digital Particle Image Velocimetry in MATLAB. *J. Open Res. Softw.* **2014**, *2*, e30, doi:10.5334/jors.bl.
7. Torres-Serra, J.; Romero, E.; Rodríguez-Ferran, A. Hygroscopicity issues in powder and grain technology. In Proceedings of the 7th International Conference on Unsaturated Soils (UNSAT2018), Hong Kong, China, 3–5 August 2018.
8. Torres-Serra, J.; Tunuguntla, D.R.; Denissen, I.F.C.; Rodríguez-Ferran, A.; Romero, E. Discrete element modelling of granular column collapse tests with industrial applications. In Proceedings of the V International Conference on Particle-based Methods—Fundamentals and Applications (PARTICLES 2017), Hannover, Germany, 26–28 September 2017; pp. 530–538.



© 2018 by the authors. Licensee MDPI, Basel, Switzerland. This article is an open access article distributed under the terms and conditions of the Creative Commons Attribution (CC BY) license (<http://creativecommons.org/licenses/by/4.0/>).